Propulsion and Power Research 2016;5(3):250–260

HOSTED BY

ELSEVIER

http://ppr.buaa.edu.cn/

Propulsion and Power Research

www.sciencedirect.com

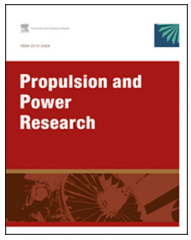

ORIGINAL ARTICLE

Interlayer shear effect on vibrational behavior of bilayer graphene using the molecular mechanics simulation

Mina Mirparizi[a], **Farshad Shakeri Aski**[b,*]

[a]*Department of Mechanical Engineering, University of Yazd, Yazd, Iran*
[b]*Department of Mechanical Engineering, Shahid Bahonar University of Kerman, Kerman, Iran*

Received 2 March 2015; accepted 29 May 2015
Available online 9 August 2016

KEYWORDS

Graphene;
Vibration;
Molecular mechanics;
Interlayer interaction;
Lennard–Jones

Abstract In this article, the interlayer shear effects on vibrational behavior of bilayer graphene (BG) are studied by using the molecular mechanics (MM) simulation. Investigation on mechanical behavior of graphenes has recently attracted because of their excellent properties. MM simulation is exploited for modeling of covalent bond in the plane of graphene layers and they are modeled as space-frame structures. The interaction between two layers is modeled by Lennard–Jones potential for not only two apposite atoms but also for all adjacent atoms. The frequencies and mode shapes for cantilever and bridged bilayer graphene as well as monolayer graphene (MG) are obtained by a finite element approach. Results show that the interlayer shear interaction has considerable effect on vibrational behavior of BG and increases the natural frequencies, because existence of horizontal forces (shear forces) that prevent the lateral displacements. It can be seen that the interaction between two layers are more considerable in second mode because the curvature and variation of displacement are higher in second mode. Also it can be found that changing of mode shapes has considerable effect on shear interaction.

1. Introduction

Graphene, an extraordinary substance, consists of carbon atoms which are connected by covalent bonds and constitute the hexagonal lattices. Graphene layers are held together by

*Corresponding author.
E-mail address: f.shakeriaski@gmail.com (Farshad Shakeri Aski).

Peer review under responsibility of National Laboratory for Aeronautics and Astronautics, China.

http://dx.doi.org/10.1016/j.jppr.2016.07.006

Nomenclature

M	mass (unit: kg)
U	potential energy (unit: J)
E	modulus of elasticity (unit: Pa)
A	cross section (unit: m^2)
G	modulus of shear (unit: Pa)
D	diameter (unit: m)
R	length of carbon bond (unit: m)
I	moment of inertia (unit: m^4)
J	polar moment of inertia(unit: m^4)
D_e	potential of bond in Morse function (unit: J)
K_r	stretching stiffness (unit: N/m)
K_Θ	bending stiffness (unit: N/m)
K_τ	torsion stiffness (unit: N/m)
V_{LJ}	Lennard-Jones potential (unit: J)

Greek letters

ω	angular frequency (unit: rad/s)
τ	shear stress (unit: Pa)
Θ	bond angles
σ	Lenard–Jones parameter
ϵ	bond energy in Lennard–Jones potential

Subscripts

MM	molecular mechanics
MG	monolayer graphene
BG	bilayer graphene

van der Waals (vdW) forces which is a weak interaction. Graphene have recently attracted many researchers for its extra properties, such as high electrical and thermal conductivities and very large Young modulus. Because of these properties, graphene is used in many fields such as in polymer composites and resonators.

The molecular mechanics method has been widely applied to study the mechanical analysis of nano-structures because its computation is faster than quantum mechanics and molecular dynamics methods. This method used by Chang and Gao [1] and Xiao et al., [2] for determination the physical properties of single-walled carbon nanotube (CNT). Avila et al. [3] studied vibration of nanotubes by using molecular mechanics (MM) approach and found that with increasing of length to radius in CNTs, the fundamental frequency decreases. Rouhi and Ansari [4] developed the axial buckling and vibration analyses of single-layered graphene sheets using MM and observed that with increasing the dimensions, the effect of boundary conditions vanishes. Large amplitude vibration analysis of multilayered graphene sheets has been described by Jomehzadeh and Saidi [5] by considering the effect of small length scale. They also decoupled the nonlocal elasticity equations for three dimensional vibration analyses of nano-plates [6]. They recently investigated nonlinear free and forced vibration of a bilayer grapheme (BG) embedded in a polymer medium [7]. Liu et al. [8] proposed a multi-beam shear model to consider interlayer shear effect and used molecular dynamics method and offered a new formulation for fundamental and secondary resonant frequencies. He et al. [9] studied vibration of multi-layered graphene sheets by continuum plate model and their results show that effect of vdW interaction on low frequency is small but it intensifies the high frequencies. Also, Liew et al. [10] studied vibration of multi-layered graphene sheets embedded in an elastic matrix and utilized the continuum model. they reported that surrounding matrix has significant effect on high frequency. Askari et al. studied nonlinear vibration analysis of nano-wires [11].

Hashemnia et al. [12] simulated carbon nanotubes and graphene sheets as space-frame structures using MM to investigate their vibration characteristics and reported the fundamental frequencies of nanotubes are greater than graphene sheets. Also, Sakhaee-Pour et al. [13] studied vibrational analysis of single-layered graphene sheets by MM simulations and calculated their fundamental frequencies in range of Terahertz. Babaei and Shahidi [14] worked on vibration of quadrilateral embedded multilayered graphene sheets and used the Galerkin method. They found that the effect of layers number is not important on lower frequencies. Finally, they extended their researches for skew, rhombic, rectangular and trapezoidal MLGS that embedded in a polymer matrix. Theodosiou and Saravanos used molecular mechanics based finite element for graphene to enable prediction of mechanical failure in graphene sheets [15]. Recently several papers were published in which authors used finite element method and lattice Boltzmann method [16–35].

In this article, the effects of interlayer shear interaction on vibration of BGs are studied. By using MM simulations, an atomistic model is prepared that can predict the shear forces of graphene layers. Finite element method is applied to obtain the natural frequencies of the system. Finally, vibration behavior of graphene with shear effects and without shear is compared.

2. Molecular mechanics simulation

Molecular mechanics or force-field method uses classical type models to predict the energy of a molecule as a function of its conformation. This allows prediction of equilibrium geometries and transition states relative energies between conformers or between different molecules [36]. Molecular mechanics, based on the Born–Oppenheimer approximation, disregards the electronic structure and expresses the energy of system, only as a function of the nuclear positions [1,37].

Atoms in graphene layers are connected together with covalent bonds. The molecular mechanic model considers atoms as concentrated mass and bonds as beams or springs with ability of stretching, bending and torsion. The explicit form of potential energy has proffered by molecular mechanics as:

$$U_{tot} = \sum U_{str} + \sum U_{bend} + \sum U_{tors} + \sum U_{vdw} + \sum U_{elec} \quad (1)$$

where U_{str} is the bond stretching energy and expresses the energy produced by extension and contraction of bonds, U_{bend} is the angle bending energy and explains the energy that stores in bond for mutation of angle from its equilibrium state and U_{tors} is the torsion potential due to rotation around the simple bond (Figure 1). U_{vdw} and U_{elec} are non-bonded energy which are related to van der Waals interaction and electrostatic energy, respectively which are short-range effects [37].

Therefore, we can determination mathematical relations for modeling of covalent bonds in form of beams (Figure 2).

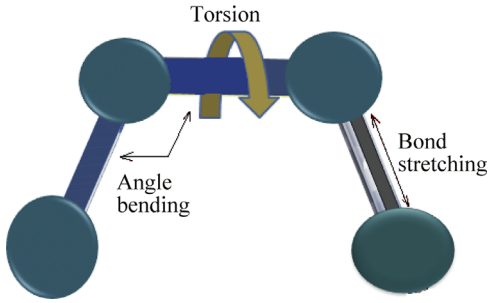

Figure 1 Interactions of carbon atom by covalent bonds.

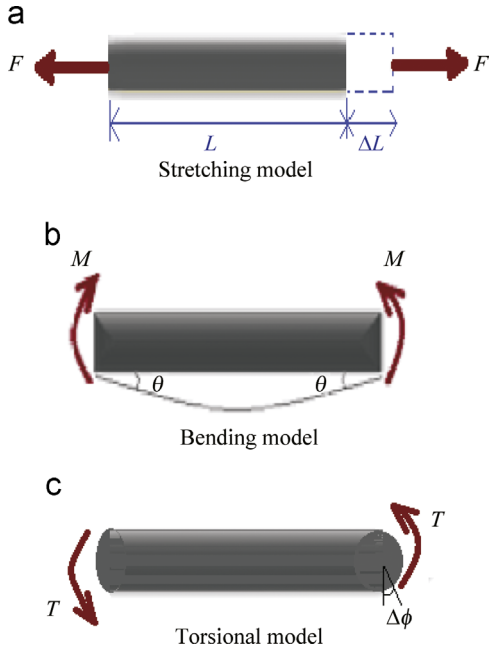

Figure 2 Substitution of beam instead of carbons bounds in molecular mechanics. (a) Stretching model, (b) bending model, and (c) torsional model.

There are several potential functions that have been utilized to express the interactions of carbon atoms. Morse potential function is one of the simplest potentials for characterization of bond energy in stretching, because of its diagram encompasses a large area of bond's manner from strong connected to separation. This function expresses the behavior of atoms in creation of chemical bond in a good agreement with quantum mechanics and experimental results [38]. The Morse function is expressed as:

$$U_{str} = D_e\{1-\exp[-a(r-r_0)]\}^2 \quad (2)$$

where r_0 is equilibrium length, a is a control parameter and D_e is the potential of bond.

Since Morse potential is rather a complex function, the Hook's law can be used for modeling the stretching of bonds. It has more simple equation than Morse potential and it has a good agreement and even coincides with Morse potential around the equilibrium state (Figure 3) [1,38]. Using the Hook's law instead of Morse potential is a suitable idea that applies in this work. According to Hook's law U_{str} is defined as [38]:

$$U_{str} = \frac{1}{2}K_r(r-r_0)^2 = \frac{1}{2}K_r(\Delta r)^2 \quad (3)$$

where k_r is the force constant as:

$$\frac{d^2U_{str}}{d^2r} = K_r \quad (4)$$

For accurate modeling, it is necessary to consider the bending and torsion of the carbon bonds. The similar functions can be applied for bending and torsional model [38,39]:

$$U_{bend} = \frac{1}{2}K_\theta(\theta-\theta_0)^2 = \frac{1}{2}K_\theta(\Delta\theta)^2 \quad (5)$$

$$U_{tors} = \frac{1}{2}K_\tau(\varphi-\varphi_0)^2 = \frac{1}{2}K_\tau(\Delta\varphi)^2 \quad (6)$$

K_θ and K_τ are the force field constants that related to bending and torsion stiffness of bond respectively, θ_0 and φ_0 are defined the equilibrium bond angles.

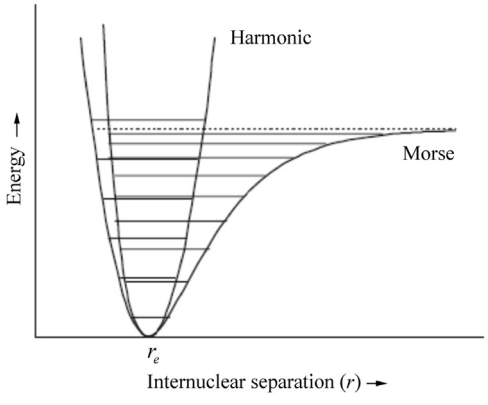

Figure 3 Morse potentials and Hook's law (harmonic function) for bond stretching [38].

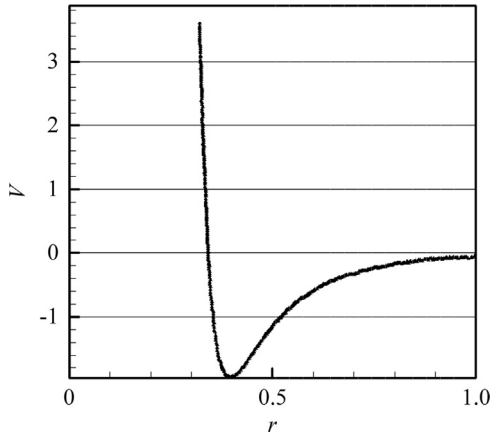

Figure 4 The van der Waals energy per distance between two atoms.

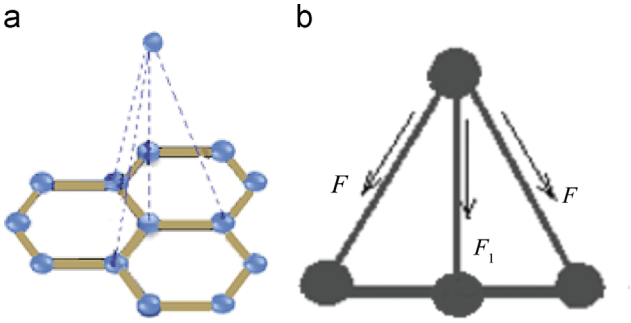

Figure 5 Atom's junction for modeling of shear effect between layers with spring element.

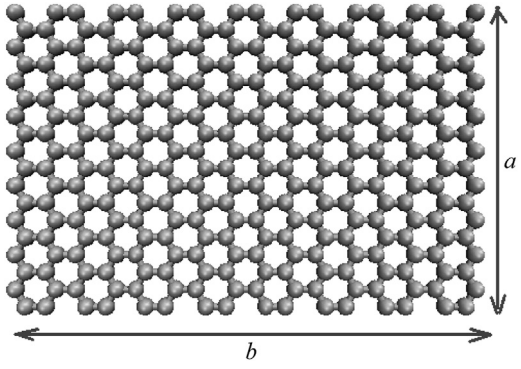

Figure 6 MG with (cfff-ccff-cccc-ssss) boundary conditions.

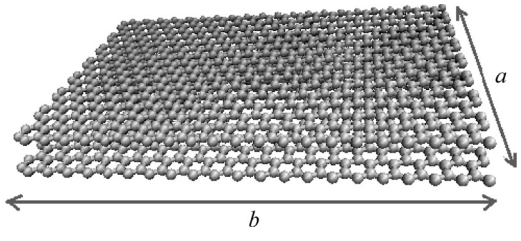

Figure 7 BG with (cfff-ccff) boundary conditions.

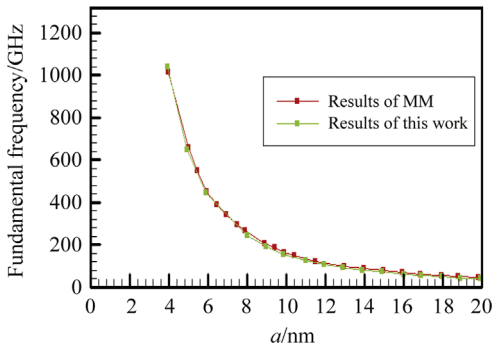

Figure 8 Comparison of fundamental frequencies of MG with clamped boundary condition and $a/b = 2.3094$.

Consider elastic beams with circular cross-section A, Young's modulus E and length L.

The relations between mechanical properties and force fields constants under pure tension, bending and twisting are obtained as [13,40]:

$$\frac{EA}{L} = K_r \tag{7a}$$

$$\frac{EI}{L} = K_\theta \tag{7b}$$

$$\frac{GJ}{L} = K_\tau \tag{7c}$$

with using Eqs. (7). Also $A = \pi d^2/4$, $I = \pi d^4/64$, $J = \pi d^4/32$ mechanical properties determined as [13]:

$$d = 4\sqrt{\frac{k_\theta}{k_r}} \tag{8}$$

$$E = \frac{K_r^2 L}{4\pi K_\theta} \tag{9}$$

$$G = \frac{K_r^2 K_\tau L}{8\pi K_\theta^2} \tag{10}$$

3. Van der Waals forces and shear effects

Interaction between pair of atoms in different graphene's layers is the van der Waals (vdW) forces that can be expressed by the Lennard–Jones 12-6 potential as:

$$V_{LJ} = 4\varepsilon\left[\left(\frac{\sigma}{r}\right)^{12} - \left(\frac{\sigma}{r}\right)^{6}\right] \tag{11}$$

In this function r^{-12}, related to repulsion between two atoms in short distance, and r^{-6} that related to attraction, in high distance intends to zero [18]. The van der Waals interaction per distance between two atoms has been shown in Figure 4.

In Lennard–Jones potential function, ε is the bond energy in equilibrium distance, and it takes the value $\varepsilon = 0.002968$ eV for carbon atoms of the graphene sheets and σ is a parameter which is determined by the equilibrium distance and its value

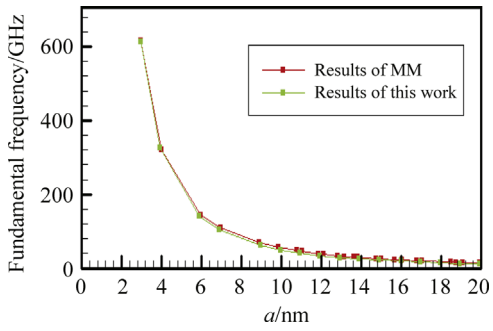

Figure 9 Comparison of fundamental frequencies of MG with clamped boundary condition and $a/b = 1.146$.

is 0.34 nm for carbon atoms [41]. Also, r is the distance between interacting atoms. The vdW force can be obtained by taking the derivative of the Lennard–Jones pair potential with respect to distance as:

$$F_{LJ} = \frac{dV_{LJ}}{dr} = 4\frac{\varepsilon}{r}\left[-12\left(\frac{\sigma}{r}\right)^{12} + 6\left(\frac{\sigma}{r}\right)^{6}\right] \tag{12}$$

element with tension, compression, torsion, and bending capabilities. The element has six degrees of freedom at each node: translations in the nodal x, y, and z directions and rotations about the nodal x, y, and z axes with six degrees-of-freedom [43]. Also COMBIN14 is applied for modeling of vdW forces, that it is a linear spring. For this frame the equation of motion is expressed as:

$$\boldsymbol{M}\{\ddot{y}\} + \boldsymbol{K}\{y\} = 0 \tag{13}$$

$\boldsymbol{M}$ and $\boldsymbol{K}$ are global mass and stiffness matrices [12]:

$$\boldsymbol{K} = \begin{bmatrix} k_{ii} & k_{ij} \\ k_{ij}^{\mathrm{T}} & k_{jj} \end{bmatrix}, \boldsymbol{M} = \begin{bmatrix} M_{ii} & M_{ij} \\ M_{ij}^{\mathrm{T}} & M_{jj} \end{bmatrix}$$

$$k_{ii} = \begin{bmatrix} EA/L & 0 & 0 & 0 & 0 & 0 \\ 0 & 12EI_x/L^3 & 0 & 0 & 0 & 6EI_x/L^2 \\ 0 & 0 & 12EI_y/L^3 & 0 & -6EI_y/L^2 & 0 \\ 0 & 0 & 0 & GJ/L & 0 & 0 \\ 0 & 0 & -6EI_y/L^2 & 0 & 4EI_y/L & 0 \\ 0 & 6EI_x/L^2 & 0 & 0 & 0 & 4EI_x/L \end{bmatrix}$$

$$k_{ij} = \begin{bmatrix} -EA/L & 0 & 0 & 0 & 0 & 0 \\ 0 & -12EI_x/L^3 & 0 & 0 & 0 & 6EI_x/L^2 \\ 0 & 0 & -12EI_y/L^3 & 0 & -6EI_y/L^2 & 0 \\ 0 & 0 & 0 & -GJ/L & 0 & 0 \\ 0 & 0 & 6EI_y/L^2 & 0 & 2EI_y/L & 0 \\ 0 & -6EI_x/L^2 & 0 & 0 & 0 & 2EI_x/L \end{bmatrix}$$

Each atom is connected not only to the opposite atom in next layer but also to the adjacent atoms of the opposite layer (Figure 5(a)).

This modeling causes the appearance of horizontal forces which can consider the shear effect between the graphene layers. The interactions of layers are simulated with spring elements and their stiffness is determined by Taylor expansion of Lennard–Jones force around equilibrium distance between layers (Figure 5(b)). This distance for vertical springs has been determined as 0.35 nm [42]. And for oblique springs is determined as 0.53 nm that it is calculated by $F = 0$. Then with Taylor expansion stiffness of vertical and oblique springs is computed as 1.659×10^{-9} N/nm and 34.56×10^{-13} N/nm, respectively.

$$k_{jj} = \begin{bmatrix} EA/L & 0 & 0 & 0 & 0 & 0 \\ 0 & 12EI_x/L^3 & 0 & 0 & 0 & -6EI_x/L^2 \\ 0 & 0 & 12EI_y/L^3 & 0 & 6EI_y/L^2 & 0 \\ 0 & 0 & 0 & GJ/L & 0 & 0 \\ 0 & 0 & 6EI_y/L^2 & 0 & 4EI_y/L & 0 \\ 0 & -6EI_x/L^2 & 0 & 0 & 0 & 4EI_x/L \end{bmatrix}$$

$$M_{ii} = M_{jj} = \begin{bmatrix} m_c & 0 & 0 & 0 & 0 & 0 \\ 0 & m_c & 0 & 0 & 0 & 0 \\ 0 & 0 & m_c & 0 & 0 & 0 \\ 0 & 0 & 0 & 0 & 0 & 0 \\ 0 & 0 & 0 & 0 & 0 & 0 \\ 0 & 0 & 0 & 0 & 0 & 0 \end{bmatrix}$$

$$M_{ij} = M_{ji} = 0$$

4. Numerical procedure for vibrational analysis of BLGSs and numerical parameter that are used

To study the vibrational behavior of BLGSs, they are modeled as space-frame structures and by using the ANSYS V12, vibrational analysis is done. BEAM4 is elected for simulation of covalent bounds. BEAM4 is a uniaxial

That have obtained by considering: $m_c = 1.9943 \times 10^{-23}$ gr (carbon nuclei mass), $k_r = 6.52 \times 10^{-7}$ N/nm, $k_\theta = 8.76 \times 10^{-10}$ Nnm/rad^2, $k_\tau = 2.78 \times 10^{-10}$ Nnm/rad^2, that are beam's constants by using Eqs. (8), (9) and (10), some parameters can be derived: $d = 1.466$ A$^\circ$, $E = 5.488 \times 10^{-8}$ N/A$^{\circ 2}$ and $G = 8.70110^{-9}$ N/A$^{\circ 2}$ [4,40].

Then the frequencies and mode shapes are obtained from the solution of the eigenvalue problem:

$$\left(\boldsymbol{K}-\omega^2\boldsymbol{M}\right)\{y\}=0 \tag{14}$$

Analysis is done for graphene with these geometrics (Figure 6 and Figure 7).

That in cfff and ccff boundary conditions, supports are set in length of a, that in BG this length related to armchair schematic, and in MG related to zigzag schematic.

5. Numerical results

At the beginning, free vibrational analysis of a MG is studied. In order to verify the accuracy of results, the fundamental natural frequency of a clamped MG is compared with MM results of Ref. [13] in Figure 8 and Figure 9 for two different aspect ratios. It can be found that the natural frequencies have a good agreement with existing results in the literature.

Fundamental frequencies of MG for two aspect ratios are depicted in Figures 10-13 for different boundary conditions. As expected, fundamental frequency of clamped graphene sheets is greater than others. Also, it can be seen that the decreasing of frequency is sharper in lower values of graphene length.

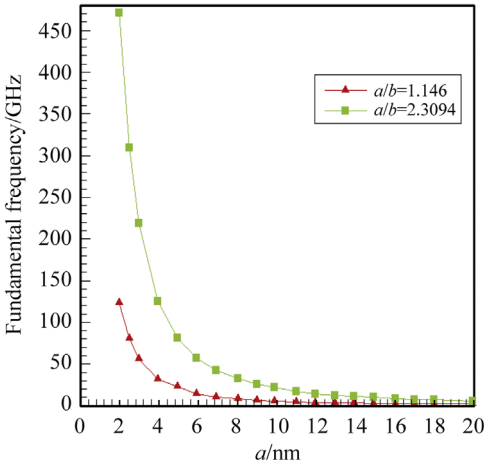

Figure 10 Fundamental frequencies of MG with one clamped edge.

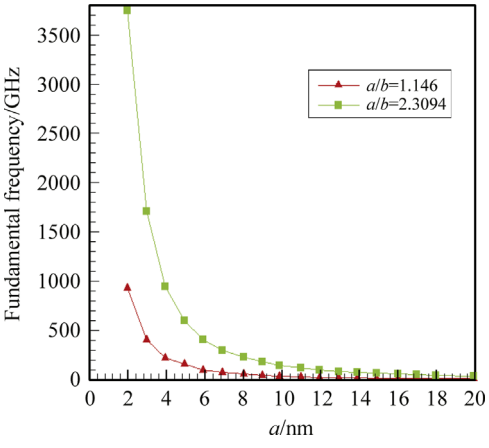

Figure 11 Fundamental frequencies of MG with two clamped edges.

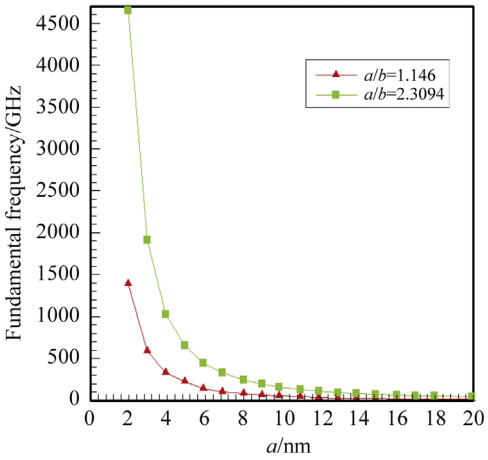

Figure 12 Fundamental frequencies of MG with four clamped edges.

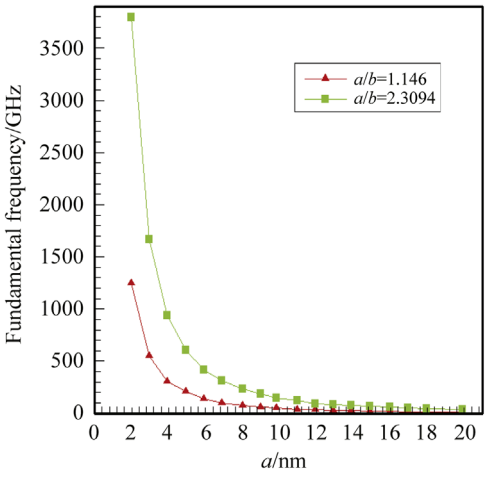

Figure 13 Fundamental frequencies of MG with four simply-supported edges.

To observe the shear effects on vibrational behavior of BG, two models are considered for vdW forces. At first model each atom of graphene layer is only connected to the opposite atom in the next layer with spring elements. In this case comparison between frequencies of MG and BG with different boundary conditions found that the fundamental frequencies of them are almost similar with same in-phase mode shapes. It shows that the springs deformations are negligible and consequently the spring elements do not affected the behavior of this model.

Therefore in this case the vdW interaction has insignificant effect on vibrational characteristics and this is not caused to a suitable result.

In second model each atom is connected to four adjacent atoms in apposite layer. First two frequencies of cantilever BG with three different widths and several lengths are presented in Table 1. ω_1 and ω_2 are first and second frequencies respectively. It can be seen that the presence of

Table 1 Comparison of cantilever BG's frequencies (GHz) in two states: with shear effect and without shear.

Dimensions		$b=2.55$ nm		$b=4.8$ nm		$b=9.7$ nm	
		ω_1	ω_2	ω_1	ω_2	ω_1	ω_2
$a=5.16$ nm	Without shear	13.796	55.377	11.834	28.056	14.309	21.907
	With shear	14.125	56.224	12.160	28.506	14.634	22.227
	Error	2.3%	1.5%	2.75%	1.6%	2.2712%	1.46%
$a=8.11$ nm	Without shear	5.7699	33.429	5.9131	18.128	5.9889	12.037
	With shear	6.0859	34.502	6.2291	18.737	6.3024	12.418
	Error	5.47%	3.209%	5.35%	3.35%	5.234%	3.165%
$a=10.08$ nm	Without shear	3.9270	22.453	4.0135	14.082	4.0634	9.2052
	With shear	4.2240	22.830	4.3117	14.809	4.3599	9.6410
	Error	7.55%	1.67%	7.429%	5.162%	7.29%	4.734%
$a=15.98$ nm	Without shear	2.1378	9.0559	2.1600	8.4653	2.1758	5.4230
	With shear	2.3473	9.4216	2.3735	9.3622	2.3895	6.0040
	Error	9.79%	4.03%	9.86%	10.59%	9.821%	10.71%
$a=19.92$ nm	Without shear	1.8386	5.9556	1.8487	6.0622	1.8560	4.3179
	With shear	1.9928	6.3088	2.0064	6.4199	2.0148	4.9354
	Error	8.38%	5.93%	8.5%	5.95%	8.556%	14.3009%
$a=25.08$ nm	Without shear	1.6952	3.9525	1.6993	4.0142	1.7022	3.4782
	With shear	1.7980	4.2812	1.8047	4.3471	1.8087	4.0627
	Error	6.06%	8.316%	6.22%	8.29%	6.256%	16.80%
$a=35.17$ nm	Without shear	1.6206	2.4334	1.6216	2.4540	1.6223	2.4725
	With shear	1.6717	2.6948	1.6740	2.7233	1.6754	2.7404
	Error	3.153%	10.74%	3.23%	10.82%	3.273%	10.835%

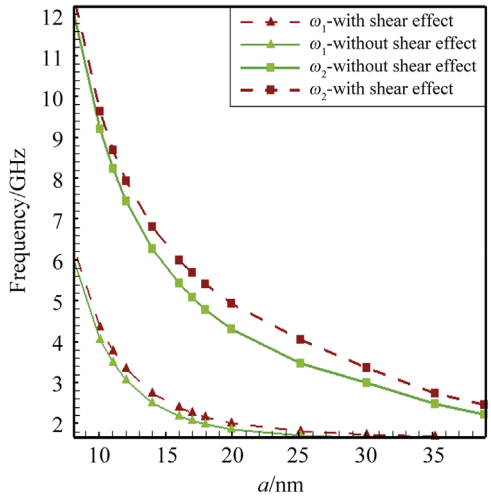

Figure 14 Effect of shear on first two frequencies of cantilever BG ($b=9.7$ nm).

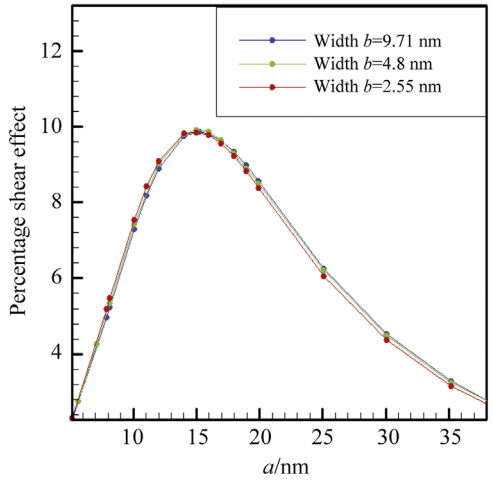

Figure 15 Variations of percentage increase in fundamental frequencies of cantilever BG.

shear effect of interaction causes increasing of the natural frequencies.

It can be observed that shear effect between layers causes a remarkable increasing in natural frequencies for some dimensions of BG.

In fact natural frequencies are increased by adding of oblique springs because creation of horizontal forces (shear forces) that prevent the lateral displacements. For better understanding of the shear effect, a comparison study is shown in Figure 14 for first and second natural frequencies of cantilever BG. It can be seen that the shear effect of vdW

Table 2 Effect of shear on fundamental frequencies (GHz) of bridged BGs and comparison of these with cantilever BGs.

Boundary conditions		$a=7.87$ nm		$a=11.08$ nm		$a=19.92$ nm		$a=35.171$ nm	
		cfff	ccff	cfff	ccff	cfff	ccff	cfff	ccff
$b=2.55$ nm	Without shear	6.109	39.70	3.377	19.84	1.838	6.198	1.620	2.478
	With shear	6.427	39.84	3.662	19.99	1.992	6.335	1.671	2.586
	Error	5.2%	0.35%	8.42%	0.71%	8.38%	2.21%	3.15%	4.33%
$b=9.71$ nm	Without shear	6.342	40.978	3.486	20.534	1.856	6.417	1.6223	2.532
	With shear	6.658	41.121	3.772	20.677	2.014	6.555	1.675	2.641
	Error	4.96%	0.34%	8.17%	0.69%	8.55%	2.14%	3.27%	4.3%

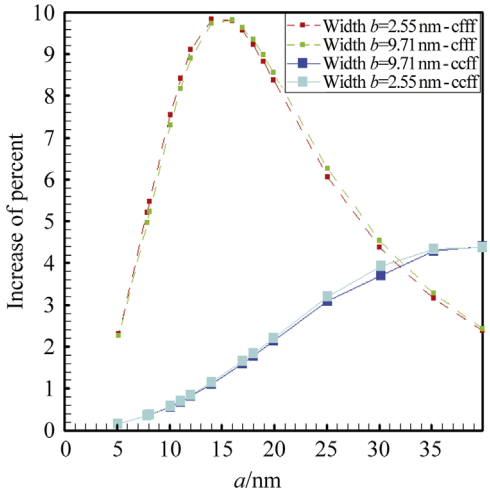

Figure 16 Comparison between variations of percentage increase in fundamental frequencies of cantilever BGs and bridged BGs.

is more considerable in second mode because the curvature and variation of displacement are higher in second mode.

As it can be seen from Table 1, frequency percentages are calculated as errors that show the changes in percentage of shear effect are not constant for different lengths. For better understanding, variation of the shear effect percentage is depicted in Figure 15 for different lengths. It can be found that for low lengths, the shear effect has a significant influence and after a specific length, the percentage of shear effect decreases.

Since the natural frequencies are increased by adding of oblique springs and in high dimensions there are more springs that cause increasing of the stiffness. However, as the dimension of the BG is increase, the effect of shear forces becomes negligible such as long beams or plates. Therefore, as it can be seen from Figure 15 there is specific dimension ($\sim a=15$ nm) in which these effects overcome each other.

The vdW shear effect on vibrational behavior of bridged BG is also investigated. Comparison between fundamental frequencies of bridged (ccff) and cantilever (cfff) BGs in two cases are shown in Table 2. It can be seen that the effect of vdW shear interaction is more considerable in small lengths of cfff BG. Also, for long lengths of ccff BG, the shear effect is significant. For more understanding, the frequency percentage versus different lengths is shown in Figure 16. It can be seen that for a specific length around $a=32$ nm, the shear effect of vdW is independent of boundary condition. Whereas in small lengths, the shear effect of vdW in cfff BG is more than ccff BG. Since the displacement of the cfff BG is more than ccff BG, adding of oblique springs for vdW shear interaction seems more effective in cfff BG. But, in long lengths, the bending effect is more considerable than the shear interaction.

The second mode shapes of BGs are shown in Table 3. By study the second frequencies of each graphene sheet in Table 3, it can be seen that when the length is increasing, the frequency percentages also increase especially in long lengths. In some points the shear effect comes down due to change of mode shapes. Comparison of each mode and its error shows that conversation of out-of-phase modes (torsion) into bending modes causes decrease of percentage. Also with increase of length the percentage is increased again. Such as $a=7.87$ nm, $b=2.55$ nm in Table 3 with conversation of out-of-phase modes in to the bending modes the percent is decreased, also in $a=10.08$ nm, $b=2.55$ nm and etc.

By investigation the effect of shear on second mode it can be seen that frequency percentages increases with growth of length. And this does not happen when the mode shape changes from torsion to bending.

Table 3 The second mode shapes of cantilever and bridged BLGS with different dimensions.

a	b=2.55 nm		b=9.71 nm	
	ccff	cfff	ccff	cfff
a=7.87 nm	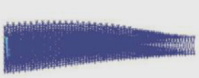 3.3%	 0.28%	 2.98%	 0.43%
a=10.08 nm	 1.67%	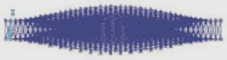 1.37%	 4.73%	 0.79%
a=12.05 nm	 2.36%	 0.42%	 6.60%	 1.23%
a=16.97 nm	 4.49%	 0.84%	 11.70%	 2.8%
a=19.92 nm	 5.93%	 1.16%	 14.30%	 4.05%
a=25.08 nm	 8.31%	 1.82%	 16.80%	 6.701%
a=35.17 nm	 10.74%	 3.36%	 10.83%	 12.65%
a=39.84 nm	 10.63%	 4.07%	 10.85%	 7.02%

6. Conclusion

The interlayer shear effects on vibrational behavior of bilayer graphene (BG) have been studied. By using molecular mechanics, graphene layers have been modeled as space-frame structures with appropriate force field. It is found that natural frequencies are increasing when the shear interactions of layers are considered. In the first mode shape of cantilever BGs that related to bending mode, can determine a specific point, that the increasing percentage of frequencies are maximized. With comparison between cantilever and bridged BGs, it is observed that there is also a specific point that before this point the shear effect in cantilever BGs is more than bridged BGs and after this

point, it is reversed. By comparison of second modes, it is found that increasing percentage of frequency is decreased with increasing of length, except in some point that related to change of mode shapes from out-of-phase mode to bending mode.

References

[1] T. Chang, H. Gao, Size-dependent elastic properties of a single-walled carbon nanotube via a molecular mechanics model, J. Mech. Phys. Solids 51 (2003) 1059–1074.

[2] J.R. Xia, B.A. Gama, J.W. Gillespie Jr, An analytical molecular structural mechanics model for the mechanical properties of carbon nanotubes, Int. J. Solids Struct. 42 (2005) 3075–3092.

[3] F. Avila Antonio, C. Eduardo Alexandre, S. Neto Almir, Vibrational analysis of graphene based nanostructures, Comput. Struct. 89 (2011) 878–892.

[4] S. Rouhi, R. Ansari, Atomistic finite element model for axial buckling and vibration analysis of single-layered graphene sheets, Physica E 44 (2012) 764–772.

[5] E. Jomehzadeh, A. RSaidi, A study on large amplitude vibration of multilayered graphene sheets, Comput. Mater. Sci. 50 (2011) 1043–1051.

[6] E. Jomehzadeh, A.R. Saidi, Decoupling the nonlocal elasticity equations for three dimensional vibration analysis of nano-plates, Compos. Struct. 93 (2011) 1015–1020.

[7] E. Jomehzadeh, A.R. Saidi, N.M. Pugno, Large amplitude vibration of a bilayer graphene embedded in a nonlinear polymer matrix, Physica E 44 (2012) 1973–1982.

[8] Y. Liu, Z. Xu, Q. Zheng, The interlayer shear effect on graphene multilayer resonators, J. Mech. Phys. Solids 59 (2011) 1613–1622.

[9] X.Q. He, S. Kitipornchai, K. Liew, Resonance analysis of multi-layered graphene sheets used as nanoscale resonators, Nanotechnology 16 (2005) 2086–2091.

[10] K.M. Liew, X.Q. He, S. Kitipornchai, Predicting nanovibration of multi-layered graphene sheets embedded in an elastic matrix, Acta Mater. 54 (2006) 4229–4236.

[11] H. Askari, E. Esmailzadeh, D. Zhang, Nonlinear vibration analysis of nonlocal nano wires, Composites Part B: Eng. 67 (2014) 607–613.

[12] K. Hashemnia, M. Farid, R. Vatankhah, Vibrational analysis of carbon nano tubes and graphene sheets using molecular structural mechanics approach, Comput. Mater. Sci. 47 (2009) 79–85.

[13] A. Sakhaee-Pour, M.T. Ahmadian, R. Naghdabadi, Vibrational analysis of single-layered graphene sheets, Nanotechnology 19 (2008) 085702.

[14] H. Babaei, A.R. Shahidi, Vibration of quadrilateral embedded multilayered graphene sheets based on nonlocal continuum models using the Galerkin method, Acta Mech. Sin. 27 (6) (2011) 967–976.

[15] T. Theodosiou, D. Saravanos, Numerical simulation of graphene fracture using molecular mechanics based nonlinear finite elements, Comput. Mater. Sci. 1 (2014) 56–65.

[16] M. Sheikholeslami, R. Ellahi, Simulation of ferrofluid flow for magnetic drug targeting using Lattice Boltzmann method, J. Z. Fur Naturforschung A, Verl. der Z. für Naturforschung 70 (2) (2015) 115–124.

[17] M. Sheikholeslami, D.D. Ganji, Hydrothermal Analysis in Engineering Using Control Volume Finite Element Method, Academic Press, Print Book ISBN: 9780128029503.

[18] M.S. Kandelousi, Effect of spatially variable magnetic field on ferrofluid flow and heat transfer considering constant heat flux boundary condition, Eur. Phys. J. (2014) 129–248.

[19] M. Sheikholeslami, D.D. Ganji, M.M. Rashidi, Ferrofluid flow and heat transfer in a semi annulus enclosure in the presence of magnetic source considering thermal radiation, J. Taiwan Inst. Chem. Eng. 47 (2015) 6–17.

[20] M.S. Kandelousi, KKL correlation for simulation of nanofluid flow and heat transfer in a permeable channel, Phys. Lett. A 378 (45) (2014) 3331–3339.

[21] M. Sheikholeslami, D.D. Ganji, Entropy generation of nanofluid in presence of magnetic field using Lattice Boltzmann method, Physica A 417 (2015) 273–286.

[22] M. Sheikholeslami, Mofid Gorji-Bandpy, Kuppalapalle Vajravelu, Lattice Boltzmann simulation of magnetohydrodynamic natural convection heat transfer of Al_2O_3-water nanofluid in a horizontal cylindrical enclosure with an inner triangular cylinder, Int. J. Heat Mass Transf. 80 (2015) 16–25.

[23] M. Sheikholeslami, Effect of uniform suction on nanofluid flow and heat transfer over a cylinder, J. Braz. Soc. Mech. Sci. Eng. (2014), http://dx.doi.org/10.1007/s40430-014-0242-z.

[24] M. Sheikholeslami, S. Abelman, D.D. Ganji, Numerical simulation of MHD nanofluid flow and heat transfer considering viscous dissipation, Int. J. Heat Mass Transf. 79 (2014) 212–222.

[25] M. Sheikholeslami, D.D. Ganji, Ferrohydrodynamic and Magnetohydrodynamic effects on ferrofluid flow and convective heat transfer, Energy 75 (2014) 400–410.

[26] M. Sheikholeslami, M. Gorji-Bandpay, D.D. Ganji, Investigation of nanofluid flow and heat transfer in presence of magnetic field using KKL model, Arab. J. Sci. Eng. 39 (6) (2014) 5007–5016.

[27] M. Sheikholeslami, M.G. Bandpy, R. Ellahi, A. Zeeshan, Simulation of MHD CuO-water nanofluid flow and convective heat transfer considering Lorentz forces, J. Magn. Magn. Mater. 369 (2014) 69–80.

[28] M. Sheikholeslami, M. Gorji-Bandpy, D.D. Ganji, S. Soleimani, Natural convection heat transfer in a nanofluid filled inclined L-shaped enclosure, IJST, Trans. Mech. Eng. 38 (2014) 217–226.

[29] M. Sheikholeslami, M. Gorji-Bandpy, D.D. Ganji, P. Rana, S. Soleimani, Magnetohydrodynamic free convection of Al_2O_3-water nanofluid considering thermophoresis and Brownian motion effects, Comput. Fluids 94 (2014) 147–160.

[30] M. Sheikholeslami, M. Gorji-Bandpy, Free convection of ferrofluid in a cavity heated from below in the presence of an external magnetic field, Powder Technol. 256 (2014) 490–498.

[31] M. Sheikholeslami, M. Gorji-Bandpy, D.D. Ganji, Lattice Boltzmann method for MHD natural convection heat transfer using nanofluid, Powder Technol. 254 (2014) 82–93.

[32] M. Sheikholeslami, M. Gorji-Bandpy, D.D. Ganji, Numerical investigation of MHD effects on Al_2O_3-water nanofluid flow and heat transfer in a semi-annulus enclosure using LBM, Energy 60 (2013) 501–510.

[33] M. Sheikholeslami, M. Gorji-Bandpay, D.D. Ganji, Magnetic field effects on natural convection around a horizontal

circular cylinder inside a square enclosure filled with nanofluid, Int. Commun. Heat Mass Transf. 39 (2012) 978–986.
[34] M. Sheikholeslami, S. Abelman, Two phase simulation of nanofluid flow and heat transfer in an annulus in the presence of an axial magnetic field, IEEE Trans. Nanotechnol. (2015), http://dx.doi.org/10.1109/TNANO.2015.2416318.
[35] M. Sheikholeslami, M.M. Rashidi, Effect of space dependent magnetic field on free convection of Fe_3O_4-water nanofluid, J. Taiwan Inst. Chem. Eng. (2015), http://dx.doi.org/10.1016/j.jtice.2015.03.035.
[36] C.D. Sherrill, Introduction to Molecular Mechanics, School of Chemistry and Biochemistry, Georgia Institute of Technology.
[37] H.D. Folkers, G. Folkers, Molecular Modeling Basic Principles and Applications, Weinheim - New York - Base1, Cambridge - Tokyo, 1996.
[38] N.L. Allinger, Molecular structure Understanding Steric and Electronic Effects from Molecular Mechanics, ⟨Isbn:978-0-470-19557-4⟩.
[39] B.R. Gelin, Molecular Modeling of Polymer Structures and Properties, Hanser/Gardner, Cincinnati, 1994.
[40] K.I. Tserpes, P. Papanikos, Finite element modeling of single-walled carbon nanotubes, Composites: Part B 36 (2005) 468–477.
[41] R.M. Lin, Nanoscale vibration characterization of multi-layered graphene sheets embedded in an elastic medium, Comput. Mater. Sci. 53 (2012) 44–52.
[42] K. Behfar, R. Naghdabadi, Nanoscale vibrational analysis of a multi-layered graphene sheet embedded in an elastic medium, Composites Sci. Technol. 65 (2005) 1159–1164.
[43] Ansys V.12, help, Beam 4.